Contribution of picophytoplankton to carbon export in the equatorial Pacific: A reassessment of food web flux inferences from inverse models

Michael R. Stukel* and Michael R. Landry

Scripps Institution of Oceanography, University of California at San Diego, La Jolla, California

Abstract

   The paradigm that carbon export is derived almost exclusively from the primary production of large phytoplankton has been challenged by inverse ecosystem modeling studies that suggest that most carbon export in the open ocean is fueled by picophytoplankton. To readdress this hypothesis, we use an inverse model to synthesize the planktonic rate measurements from a pair of recent cruises in the equatorial Pacific. The analysis based on this new experimental data, which crucially include vertically integrated taxon-specific production and grazing estimates, largely resolve the unexpected results of the previous inverse studies, including unbalanced growth and grazing processes and the dominance of production by picophytoplankton. While this very small size class does not produce the majority of phytoplankton carbon that is eventually exported to depth (only 23%, vs. 73% from a previous analysis of Joint Global Ocean Flux Study Equatorial Pacific data), our base model supports the conclusion that the role of picophytoplankton in vertical carbon flux is largely proportional to their contribution to net primary productivity (though neither is proportional to biomass). We show, however, that export-production proportionality is sensitive to the model representation of the detrital pool such that the relative export role of picophytoplankton declines substantially for an alternate model with size-structured detritus. A definitive assessment of the role of picoplankton in vertical carbon flux will thus require detailed experimental examination of the origin, composition, and fate of euphotic zone detrital material.

   Small photosynthetic organisms (*Prochlorococcus*, *Synechococcus*, and picoeukaryotes) with cell sizes < 2 μm diameter, collectively called the picophytoplankton, are abundant and important primary producers, especially over the vast tropical and subtropical regions of the ocean (Li et al. 1983; Takahashi and Bienfang 1983). Conventional wisdom holds that these picophytoplankton are too small to sink individually or to be exploited efficiently by most metazooplankton but rather are consumed and largely respired in the euphotic zone by protistan consumers. Indeed, a good deal of experimental evidence from the ocean points to a close balance between picophytoplankton production and grazing losses to protists (Brown et al. 1999; Landry et al. 2003; Hirose et al. 2008), analogous to the tightly coupled growth–grazing–recycling processes of the "microbial loop" that are presumed to dissipate most of the matter and energy produced by heterotrophic bacteria (Azam et al. 1983). If this is the case, the amount of picophytoplankton production that ultimately leaves the euphotic zone as exported carbon should be disproportionately small compared to export that originates as larger phytoplankton, which have more direct pathways to aggregate sinking and utilization by large pellet-producing zooplankton.

   This conventional paradigm has been challenged recently in a series of papers (Richardson et al. 2004, 2006; Richardson and Jackson 2007) that have applied inverse modeling techniques to data sets derived from intensive investigations by the US Joint Global Ocean Flux Study (JGOFS) in the equatorial Pacific and the Arabian Sea. As synthesized in Richardson and Jackson (2007), these inverse analyses support two general conclusions regarding the relationship between picophytoplankton and export in open-ocean systems. The first is that the picophytoplankton contribution to vertical carbon export by sinking particles from direct and indirect pathways is a high fraction of the community total, averaging 73% of export (SD = 21%; their table 1) across a broad range of seasonal and environmental conditions in the two major ecosystems examined. The second is that the picophytoplankton contribution to export is proportional to their contribution to net primary production. The proportionality hypothesis implies that the large percentage contribution of picophytoplankton to total flux derives mainly from their dominance of primary production. Whether picophytoplankton dominate production emerges as a separate question, as does the relationship between biomass and production, since Richardson et al. (2004, 2006) use size-class contributions to total phytoplankton biomass as a proxy for their relative contributions to net production rate.

   Methodological considerations limit our ability to assess directly the actual contributions of large and small phytoplankton to export flux. However, picophytoplankton have been found in sediments, transported there by phytodetrital aggregates (Lochte and Turley 1988) or salp fecal pellets (Pfannkuche and Lochte 1993). Picoplankton-containing aggregates (Waite et al. 2000) and zeaxanthin (Lamborg et al. 2008) have also been caught in sediment traps, although both may be derived from unassimilated grazing on picophytoplankton (Gorsky et al. 1999; Waite et al. 2000). Nonetheless, the few studies that directly compare the flux of large and small phytoplankton (Silver and Gowing 1991; Rodier and Le Borgne 1997) typically find intact picophytoplankton to be only a small proportion of total carbon flux.

* Corresponding author: mstukel@ucsd.edu

In a recent synthesis of food web fluxes in the Arabian Sea, Landry (2009) found that the JGOFS data for that region was consistent with a more conventional analysis of process rates and relationships than suggested by inverse methods. In particular, Landry (2009) highlighted potential problems in the model inputs for primary production, which were partitioned proportionately among size classes according to filter-fractioned chlorophyll, a method that could inflate the smallest (picophytoplankton) class due to the extrusion of larger cells (or chloroplasts from broken cells) through the 2-μm-filter pores. Based on size-fractioned chlorophyll, picophytoplankton made up 70%, on average, of primary production for the seasons and stations that were modeled. According to microscopic and flow-cytometric assessments from the same Arabian Sea cruises and stations (Garrison et al. 2000), however, picophytoplankton made up only 35% of the total phytoplankton carbon biomass. Therefore, if production had been assumed to scale with carbon rather than size-fractioned chlorophyll, the ratio of modeled carbon flows originating from small and large cells would have decreased by a factor of four, likely affecting the behaviors of many pathways in the trophic network. In addition, the concept of proportionality in small cell contribution to export was enhanced in the Richardson et al. (2004, 2006) inverse models by an uncoupled growth-grazing condition that drove a large ungrazed fraction of picophytoplankton production directly to detritus. This growth-grazing imbalance was not, in fact, evident in the experimental data (Verity et al. 1996b) but arose rather from a decision to scale up computed taxon-specific phytoplankton growth rates to match ^{14}C-primary production (^{14}C-PP) without adjusting the corresponding estimates of microzooplankton grazing rates.

Here we use an inverse ecosystem modeling approach to re-examine the question of picophytoplankton contribution to export flux in the equatorial Pacific. One important aspect of our analysis is the use of recent data from a pair of cruises in the eastern equatorial Pacific in December 2004 and September 2005. Whereas the JGOFS Equatorial Pacific (EqPac) results available to Richardson et al. (2004) were an assortment of independent rates lacking vertical resolution and with virtually no microscopy for estimating carbon biomass values of phytoplankton and protozoans, the new data provide contemporaneous production, growth, and grazing rates and microscopical biomass estimates, all integrated for the full euphotic zone at a large number (31) of stations. This unprecedented assemblage of biomass and rate data allows us to rigorously constrain the net production (biomass growth) contributions of major phytoplankton taxa as model input. We further improve the analysis using variability in the field-measured ratio of gross primary production (GPP) to ^{14}C-PP to bound the GPP term by using a random walk (RW) technique to explore all possible solutions to the model terms and their statistics and by comparing results to an alternative model structure that accounts for different fates in a size-structured detrital pool. We illustrate that picophytoplankton production is an important but clearly not dominant source of carbon export in the equatorial Pacific and that conclusions about the direct and indirect contributions of picophytoplankton to export vary substantially, depending on whether the model considers size-structured detritus. We also show that the generally used minimum norm solution significantly underestimates the flows of carbon to bacteria and that an unstructured detrital pool significantly understates the export role of mesozooplankton. Further advances will require experimental studies that explicitly address the source, composition, and fate of detritus in the euphotic zone.

Methods

To best compare our results to those of Richardson et al. (2004), we used a similar construction and physiological constraints (explained in detail here) for our base ecological model (ECO) while incorporating the data (including group-specific growth and grazing) from the new cruises. As noted previously, we expanded the analysis of the model results beyond Richardson et al. (2004) by generating confidence intervals for all model outputs (using a Monte Carlo technique) and by using an RW technique to explore the solution space. In addition, we formatted and ran an alternative size-fractionated detritus model construct that incorporates a size-structured detrital pool.

Sampling and data—Model inputs and constraints on biomass structure, primary production, nitrate uptake, phytoplankton growth, and micro- and mesozooplankton grazing came from data collected on Equatorial Biocomplexity cruises EB04 (December 2004) and EB05 (September 2005) in the eastern equatorial Pacific (Table 1). Each cruise included an east–west and a north–south transect of sampling stations within the region of 110–140°W and 4°N–4°S (Fig. 1). Transit times between stations were set to allow for collecting a coherent set of plankton biomass and daily rate measurements at each station on the same schedule each day. Analyses of the resulting euphotic-zone integrated data demonstrated remarkably low variability, with coefficients of variation of only 31%, 33%, 43%, and 32% of the mean estimates for ^{14}C-PP, phytoplankton-specific growth rate, microzooplankton grazing, and mesozooplankton grazing, respectively (Balch et al. 2010; Décima et al. 2010; Landry et al. 2010). We therefore pooled measured rates and standing stocks from all stations on both cruises to compute composite averages for the region (n = 31 stations; Table 1) over a significantly broader spatiotemporal scale than that of Richardson et al. (2004).

Phytoplankton growth and microzooplankton grazing rates were determined from pairs of two-point dilution experiments conducted for eight sampling depths spanning the euphotic zone (to 0.1% of surface irradiance) at each station (Selph et al. 2010). These experiments were incubated for 24 h in seawater-cooled deck incubators at light levels representing 0.1%, 0.8%, 5%, 8%, 13%, 31%, 52%, and 100% of incident solar irradiance, corresponding to light levels at the depth of sample collection. Taxon-specific rates were determined by either high-pressure liquid chromatography pigment analysis (divinyl chlorophyll *a*

Table 1. Experimental inputs to the base ECO model. Table gives the measured mean rates and biomasses ($\pm$95% confidence limits) from the EB04 and EB05 cruises. Equations relate the measured rates to the model compartments: diatoms (DIA), other eukaryotic autotrophs (AUT), cyanobacteria (CYA), heterotrophic picoflagellates (HPF), heterotrophic nanoflagellates (HNF), heterotrophic microzooplankton (MIC), mesozooplankton (MES), bacteria (BAC), detritus (DET), and dissolved organic carbon (DOC). Flows are written as SOURCEtoSINK, from the first carbon pool to the second; gDI, gAU, and gCY are gross primary production of the three phytoplankton groups.

Rates	Equation	Value	Source
DiaNPP	gDItoDIA−DIAtoRES−DIAtoDOC	156$\pm$54 mg C m^{-2} d^{-1}	Landry et al. (2010)
AutNPP	gAUtoAUT−AUTtoRES−AUTtoDOC	505$\pm$95 mg C m^{-2} d^{-1}	Landry et al. (2010)
CyaNPP	gCYtoCYA−CYAtoRES−CYAtoDOC	203$\pm$38 mg C m^{-2} d^{-1}	Landry et al. (2010)
Diamzoogr	DIAtoHNF+DIAtoMIC	83$\pm$28 mg C m^{-2} d^{-1}	Landry et al. (2010)
Autmzoogr	AUTtoHNF+AUTtoMIC	316$\pm$67 mg C m^{-2} d^{-1}	Landry et al. (2010)
Cyamzoogr	CYAtoHPF+CYAtoHNF+CYAtoMIC	203$\pm$36 mg C m^{-2} d^{-1}	Landry et al. (2010)
Mzoogr	DIAtoMES+AUTtoMES	217$\pm$41 mg C m^{-2} d^{-1}	Décima et al. (2010)
NewProd	DOCtoEXT+DETtoEXT+MEStoEXT	F-rat$\times$NPP	
Other parameters			
C-14PP		672$\pm$73 mg C m^{-2} d^{-1}	Balch et al. (2010)
F-Rat		0.22$\pm$0.05	Parker et al. (2010)
BioHpf		12$\pm$3.9 mg C m^{-2}	Taylor et al. (2010)
BioHnf		242$\pm$39.7 mg C m^{-2}	Taylor et al. (2010)
BioMic		78.6$\pm$17.8 mg C m^{-2}	Parker et al. (2010)
BioMes		994$\pm$77 mg C m^{-2}	Décima et al. (2010)
BioBac		679$\pm$53.5 mg C m^{-2}	Parker et al. (2010)

[Chl *a*] was considered representative of *Prochlorococcus*, fucoxanthin of diatoms, and monovinyl Chl *a* of total eukaryotic phytoplankton) or flow cytometry samples (*Prochlorococcus* and *Synechococcus*; Selph et al. 2010). Pigment-derived rates were corrected for systematic changes in cellular pigment content during incubation using the initial and final experimental samples to assess the changes in the mean ratios of accessory pigment to microscopical assessments of phytoplankton biomass (e.g., fucoxanthin : diatom C). Taxon-specific estimates of production rates were determined from specific growth rates and carbon biomass according to Landry et al. (2000) and integrated
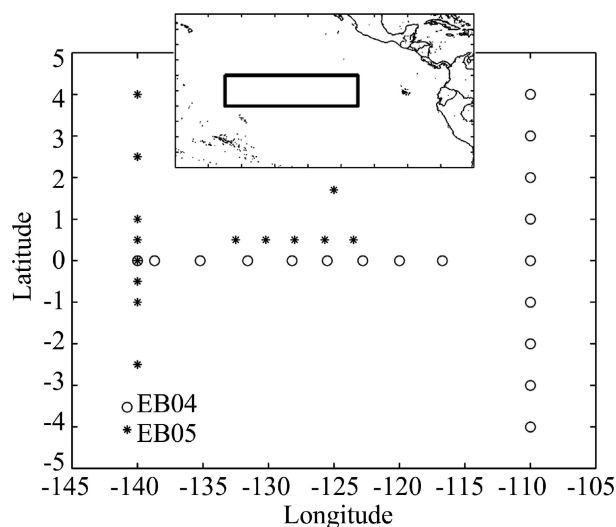

Fig. 1. Station locations for EB04 (December 2004) and EB05 (September 2005) cruises. Inset shows the study region within the greater eastern tropical Pacific from 160°W to 70°W and 25°S to 25°N.

for the full euphotic zone (Landry et al. 2010) Carbon biomass estimates of nano- and microphytoplankton were determined from the biovolumes of cells measured by epifluorescence microscopy (Taylor et al. 2010) and biovolume : carbon ratios (Menden-Deuer and Lessard 2000). Carbon biomass estimates of picophototrophs were determined from flow-cytometric analyses of cell abundances and cellular carbon content estimates (Garrison et al. 2000; Brown et al. 2008; Taylor et al. 2010). For the sake of the present analysis, we divide the phytoplankton community into cyanobacteria, diatoms, and other eukaryotic phytoplankton, the three groups that could be differentiated most easily both in epifluorescence microscopy (flow cytometry for picoplankton) and in pigment analysis. For simplicity, we do not distinguish eukaryotic picophytoplankton from other eukaryotes in this analysis, although we did microscopically and experimentally in results from the shipboard studies. True < 2-μm picoeukaryotes made up a small fraction of the autotrophic carbon pools (2% of total eukaryotes and 7% of the total < 2-μm size class; Taylor et al. 2010) and were therefore deemed to be inconsequential to the major pathways of carbon flux. Picoeukaryotes were also determined experimentally to have the same dynamics as the cyanobacteria (i.e., a close balance between production and grazing by protistan consumers; Landry et al. 2010); therefore, the flux behaviors of *Synechococcus* and *Prochlorococcus* were representative of this group.

Rates of ^{14}C-PP were measured in shipboard incubations of triplicate 250 mL samples from six discrete light levels spanning the euphotic zone (Balch et al. 2010). The *f*-ratio (ratio of new to total production) was determined by Parker et al. (2010) from measured uptake rates of ^{15}NO$_3^-$ and ^{15}NH$_4^+$. Landry et al. (2010) determined that the depth pattern and magnitudes of primary production rates from

[14]C-PP measurements and dilution growth rates were strongly related, with euphotic-integrated dilution calculations exceeding ^{14}C-PP by 29%, approximately the percentage difference observed when 12-h daytime incubations were compared to full 24-h incubations by the ^{14}C method (mean = 21%, SD = 6%; Dickson et al. 2001).

Mean daily estimates of mesozooplankton grazing rates on the bulk phytoplankton community were determined by Décima et al. (2010) from gut pigment analyses of the animals caught in paired day–night oblique plankton tows (202-μm mesh) at each station and the gut throughput estimates of Zhang et al. (1995). Mesozooplankton biomass was determined from size-fractioned dry weights (dry wt) from the same net tows, converted to carbon equivalents using the C:dry wt conversion factors in Landry et al. (2001). In synthesizing the production, growth, and grazing results of the EB cruises, Landry et al. (2010) demonstrated that euphotic zone–averaged growth rates of the phytoplankton community were balanced by the combined grazing effects of micro- and mesozooplankton, resulting in a -0.01 ± 0.11 d^{-1} net residual growth rate for the 31 stations sampled. The community rate dynamics therefore conform to expectations that the system largely functions as a steady-state chemostat (Frost and Franzen 1992; Dugdale and Wilkerson 1998). The EB cruise results therefore provide a well-integrated and strongly constrained data set for the equatorial Pacific system that includes plankton standing stocks, production, and grazing rates for the full euphotic zone.

Bacterial production (BP) and GPP were not measured on the EB04 and EB05 cruises. However, both rates showed strong correlations with ^{14}C-PP during the JGOFS EqPac cruises. BP was a relatively low proportion of primary productivity (cruise averages of 10–22%; Ducklow et al. 1995; Kirchman et al. 1995). Using the [18]O isotope method, Bender et al. (1999) showed that GPP varied from 1.9 to 2.6 times the concurrently measured rate of ^{14}C-PP. We used these field-derived relationships to set upper and lower bounds on the ratios of BP:[14]C-PP and GPP:[14]C-PP. For export, we chose not to constrain the rate of particulate organic carbon (POC) flux with EqPac data since a goal of our model was to compare POC cycling estimates to those from the EqPac study (Richardson et al. 2004); hence, we did not want to force similarities between the two models in this specific area.

Model structure—To accommodate differences in data collection between EqPac and EB cruises but staying as close as we could to the Richardson et al. (2004) structure, we divided the phytoplankton community into three taxonomic groups (diatoms, other eukaryotic autotrophs, and cyanobacteria—*Synechococcus and Prochlorococcus*) and included four size classes of grazers (pico- and nanoflagellates, microzooplankton, and mesozooplankton), as shown in Fig. 2. Grazers were allowed to graze on all equal or smaller size classes of organisms (and detritus) with the exception of the mesozooplankton, which were assumed unable to feed efficiently on picoplankton ($< 2~\mu$m) including cyanobacteria, heterotrophic picoflagellates, and heterotrophic bacteria. All biological compartments con-
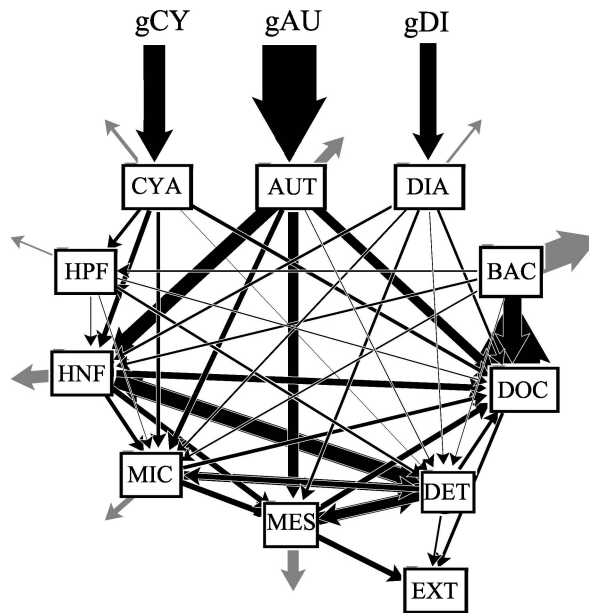

Fig. 2. Schematic representation of our model. Arrow widths are proportional to the carbon flows between any two compartments. Light gray arrows that do not end at any compartment represent respiration. Results are the mean values of an RW exploration of the solution space; gCY, gDI, and gAU are gross primary production of cyanobacteria, diatoms, and other eukaryotic autotrophs, respectively. Compartments are cyanobacteria (CYA), diatoms (DIA), other eukaryotic autotrophs (AUT), bacteria (BAC), dissolved organic carbon (DOC), detritus (DET), mesozooplankton (MES), microzooplankton (MIC), heterotrophic nanoflagellates (HNF), and heterotrophic picoflagellates (HPF). EXT is flux of carbon out of the ecosystem through consumption by higher predators, vertical flux of detritus, or lateral advection of DOC.

tributed to the dissolved organic carbon (DOC) pool through excretion and to the detrital pool via nongrazer related death (for phytoplankton and bacteria) and egestion of fecal matter (for grazer groups).

As in Richardson et al. (2004), standing stocks of the eight biological compartments in the model, as well as the two nonliving compartments (detritus and DOC), were constrained to steady-state conditions (Table 2). This assumption is supported by the demonstrated balance between growth and grazing processes in the region (Landry et al. 2010). Phytoplankton group-specific rates of growth and grazing from dilution experiments and the grazing rates of mesozooplankton were used as model constraints (Table 1). Since vertical flux rates were not measured on the cruises, we also required that combined export processes (vertical flux of detrital carbon, horizontal export of DOC away from the equator, and consumption of mesozooplankton by higher trophic levels) match the level of new production within the system, assuming similar N:C ratios for phytoplankton, mesozooplankton, detritus, and labile DOC. While shallow-water nitrification has called into question the use of nitrate uptake as a proxy for new production in low-nitrate systems (Yool et al. 2007), it is probably insignificant in the high-nitrate, upwelling region of the equatorial Pacific.

Table 2. Steady-state equations for the base ECO model. Flows and model conventions are the same as in Table 1.

Parameter	Steady-state equation
DIA	gDItoDIA−DIAtoRES−DIAtoHNF−DIAtoMIC−DIAtoMES−DIAtoDET−DIAtoDOC
AUT	gAUtoAUT−AUTtoRES−AUTtoHNF−AUTtoMIC−AUTtoMES−AUTtoDET−AUTtoDOC
CYA	gCYtoCYA−CYAtoRES−CYAtoHPF−CYAtoHNF−CYAtoMIC−CYAtoDET−CYAtoDOC
HPF	CYAtoHPF+BACtoHPF+DETtoHPF−HPFtoHNF−HPFtoMIC−HPFtoRES−HPFtoDET−HPFtoDOC
HNF	DIAtoHNF+AUTtoHNF+CYAtoHNF+HPFtoHNF+BACtoHNF+ DETtoHNF−HNFtoMIC−HNFtoMES−HNFtoRES−HNFtoDET−HNFtoDOC
MIC	DIAtoMIC+AUTtoMIC+CYAtoMIC+HPFtoMIC+HNFtoMIC+BACtoMIC+DETtoMIC− MICtoMES−MICtoRES−MICtoDET−MICtoDOC
MES	DIAtoMES+AUTtoMES+HNFtoMES+MICtoMES+DETtoMES−MEStoRES−MEStoDET− MEStoDOC−MEStoEXT
BAC	DOCtoBAC−BACtoHPF−BACtoHNF−BACtoMIC−BACtoRES−BACtoDET−BACtoDOC
DET	DIAtoDET+AUTtoDET+CYAtoDET+HPFtoDET+HNFtoDET+MICtoDET+MEStoDET+BACtoDET− DETtoHPF−DETtoHNF−DETtoMIC−DETtoMES−DETtoDOC−DETtoEXT
DOC	DIAtoDOC+AUTtoDOC+CYAtoDOC+HPFtoDOC+HNFtoDOC+MICtoDOC+MEStoDOC+BACtoDOC+ DETtoDOC−DOCtoBAC−DOCtoEXT

We further constrained the solution by requiring that the flows obey the same suite of biological inequalities (Table 3) used in the EqPac model (Richardson et al. 2004). Respiration for phytoplankton groups was allowed to vary from 5% to 30% of group GPP, while bacteria and grazers were required to respire a minimum of 20% of ingested carbon and a maximum set by an allometrically scaled specific respiration rate (*see* Table 3 for all biological constraints). DOC excretion was set to 2–55% of net primary production (NPP) for phytoplankton groups and between 10% of ingestion and 100% of respiration for grazers. Assimilation efficiencies for grazers were allowed to vary between 50% and 90% and gross growth efficiencies (GGE) between 10% and 40% (10–50% GGE for bacteria). As noted previously, we used experimentally determined relationships from EqPac cruises to constrain BP to 10–22% of ^{14}C-PP (Ducklow et al. 1995; Kirchman et al. 1995) and GPP to 190–260% of ^{14}C-PP (Bender et al. 1999).

Model solution and statistical analyses—Even with the many biological constraints on the solution space described previously, there remain an infinite number of possible solutions. To choose among these possibilities, we used the minimum norm technique of Vézina and Platt (1988) and a modified version of the MATLAB code of Jackson et al. (2001). Briefly, the method uses the singular value decomposition (SVD) to solve explicitly for the equalities (Ax = b). The SVD decomposes the A matrix into three matrices (A = U × L × V^T). The rank of the problem (less than or equal to the number of equalities) determines the number of vectors from the V matrix that are necessary to satisfy the equalities, while the remaining vectors form an orthonormal basis that can be added or subtracted to the solution while still satisfying the equality. These remaining vectors are used to find a solution that minimizes the L_2 norm while satisfying the inequality constraints (Gx ≥ h). While this minimization scheme can be seen as a mathematically parsimonious approach, there is no a priori reason that it should approximate the ways in which ecosystems are constructed. Hence, other minimization schemes may be equally valid.

To determine model sensitivity to cruise measurements (rates and standing stocks), we used the measurement means and their 95% confidence intervals to generate normal distributions for each variable. We then ran 100,000 simulations, during which we allowed the inputs to vary simultaneously by drawing them randomly from their respective distributions to generate confidence intervals for all model outputs. When possible, we utilized the full-rank inverse solution; where not, we followed the method of Olsen et al. (2006), selecting the highest-rank solution that satisfied the constraints.

The confidence intervals derived from the previously described method address errors associated only with the measurements, not with the model construction or the minimization scheme. To assess errors associated with our choice of minimization scheme, we used an RW algorithm, inspired by Kones et al. (2009), to sample the solution space of our inverse problem. We drew random samples from a uniform distribution of the orthonormal set of vectors created by the SVD and added them to our minimum norm solution. By definition, this produces solutions that satisfy the equality constraints (Ax = b). After each solution jump, we checked that the new solution also satisfied the inequality constraints (Gx ≥ h). If true, the new solution was used as a starting point for the next iteration, thus allowing an RW sampling of the entire solution space (the ensemble of solution vectors that satisfy both equality and inequality constraints).

Ecosystem parameters—One of the great powers of constructing flux networks using inverse techniques is the ability to quantify indirect flows through the ecosystem. If G is the normalized production matrix, depicting the percentage of a compartment's carbon flow that originates from each of the other compartments, and I is the identity matrix, then the matrix $(I-G)^{-1}$ gives the normalized amount of energy (direct and indirect) that a compartment derives from any other compartment. Multiplying the rows of this matrix by the total energy of the compartments gives the amount of energy a compartment derives indirectly or directly from any other compartment (Hannon 1973). This

Table 3. Minimum and maximum biological constraints on the model solution. All units are mg C m^{-2} d^{-1}. MN and RW are constraint values for the minimal L_2-norm (MN) solution and the mean of the RW exploration of the solution space (RW). Values in bold indicate that the model chose either a maximum or a minimum allowable value for the parameter. * indicates percent of ingestion. ** indicates percent of respiration. W is the characteristic size of each group of organisms and is used for allometric determination of respiration rates. For consistency, Ws of 0.02, 7.5, 2047, and 3,800,000 pg C cell^{-1} were taken from Richardson et al. (2004) for heterotrophic bacteria, heterotrophic nanoflagellates, microzooplankton, and mesozooplankton, respectively. For heterotrophic picoflagellates, a W of 0.17 pg C cell^{-1} was obtained from Taylor et al. (2010).

Rate	Population	Minimum	Maximum	MN	RW
GGE	HPF	10%	40%	24%	28%
	HNF	10%	40%	**10%**	24%
	MIC	10%	40%	27%	25%
	MES	10%	40%	**10%**	17%
	BAC	10%	50%	36%	16%
Assimilation efficiency	HPF	50%	90%	**90%**	69%
	HNF	50%	90%	**90%**	68%
	MIC	50%	90%	**90%**	66%
	MES	50%	90%	**90%**	66%
Respiration	DIA	5% GPP	30% GPP	**30%**	20%
	AUT	5% GPP	30% GPP	11%	20%
	CYA	5% GPP	30% GPP	**30%**	20%
	HPF	20% ingestion	$1.7W^{-0.25}\times e^{(0.0693(T-20))}\times\text{biomass}=45$	55%*=**45**	25%*=38
	HNF	20% ingestion	$1.7W^{-0.25}\times e^{(0.0693(T-20))}\times\text{biomass}=352$	70%*=280	29%*=197
	MIC	20% ingestion	$1.7W^{-0.25}\times e^{(0.0693(T-20))}\times\text{biomass}=114$	52%*=**114**	25%*=96
	MES	20% ingestion	$14W^{-0.25}\times e^{(0.0693(T-20))}\times\text{biomass}=446$	70%*=253	32%*=179
	BAC	20% ingestion	$1.7W^{-0.25}\times e^{(0.0693(T-20))}\times\text{biomass}=4838$	64%*=121	51%*=423
Excretion	DIA	2% NPP	55% NPP	52%	31%
	AUT	2% NPP	55% NPP	**2%**	29%
	CYA	2% NPP	55% NPP	24%	31%
	HPF	10% ingestion	100% respiration	11%*=20%**	17%*=68%**
	HNF	10% ingestion	100% respiration	**10%***=14%**	16%*=54%**
	MIC	10% ingestion	100% respiration	11%*=9%**	16%*=36%**
	MES	10% ingestion	100% respiration	**10%***=14%	17%*=52%**
Ingestion	MES	—	$3.6W^{-0.25}\times e^{(0.0693(T-20))}\times\text{biomass}=2006$	361	556
	BAC	—	$63W^{-0.25}\times e^{(0.0693(T-20))}\times\text{biomass}=10{,}246$	189	829

technique, as applied in the network analysis approach (Ulanowicz and Kay 1991) used by Richardson et al. (2004), allowed us to compare the relative importance of different biological groups to export of carbon out of the ecosystem. We also calculated the equivalent trophic level of each group, using the convention that detritus, DOC, and phytoplankton have a trophic level of one and that all other groups have a trophic level equal to one plus the sum of the trophic levels of their prey multiplied by the proportion of their diet made up of that nutritional resource (following Christensen and Pauly 1992).

Alternative model structure with size-fractionated detritus—Assessing biases in calculated flows that result from the choice of model structure is difficult because ecosystems can be described in many ways. For evaluating the origins of system export, however, one obvious oversimplification of the base ECO model is the uniform treatment of detrital carbon, implicitly assuming complete and immediate aggregation and disaggregation of all detritus. While it is reasonable to assume that all carbon entering a biological compartment will be treated similarly when utilized by a metabolic pathway, the detrital pool contains no such averaging effect. Rather, one intuitively expects that the carbon associated with a dead cyanobacterium should behave very differently than a fecal pellet with regard to its probability of contributing to export. To address how such differences affect model outputs, we created an alternative model structure with size-fractionated detritus (hereafter referred to as model SF-Det) that did not allow detrital aggregation.

In SF-Det, the detrital pool is split into pico-, nano-, and microdetritus pools. The cyanobacteria and bacteria that die as individual cells can contribute only to the picodetritus, while the other phytoplankton can flow to either the nano- or the microdetritus compartments. Grazers contribute fecal pellets to the detrital pool smaller than themselves (e.g., heterotrophic nanoflagellates produce picodetritus) with the exception of the heterotrophic picoflagellates, which produce picodetritus. Grazers were allowed to feed on detrital size classes their own size or smaller, with the exception of the mesozooplankton, which again could not feed on pico-sized particles. We allowed vertical export of both nano- and microdetritus but not picodetritus, as 0.2–2-μm particles are generally considered to be nonsinking colloids.

Results

Our results are presented in the following four sections. In the first, we use the least minimum norm (MN) solution to directly compare our model results to the EqPac model

of Richardson et al. (2004). We then consider the uncertainties introduced into the model by errors in the measured ecological data, which raises some issues with the MN solution. In the third section, we use an RW assessment of the solution space to demonstrate the range of values allowed by the model and to show that the MN norm is not representative of the wider solution space. We then use the alternative model structure with size-fractionated detritus to show that a slightly more complex model does not significantly change the structure of the biological components of the ecosystem but does give a more realistic assessment of the flux of sinking detritus to depth.

MN results and comparison to JGOFS EqPac—To compare with the JGOFS EqPac results of Richardson et al. (2004), we determined the model solution that minimized the L_2 norm. This MN solution minimizes the summed squares of all the flows but tends to simultaneously set minor flows to zero and minimize the largest flows in the model.

The use of average rate and biomass measurements from the EB cruises allows us to model composite averages of the flows in the eastern equatorial Pacific (Table 4). Production is dominated by the nondiatom eukaryotic phytoplankton of our "AUT" category (Fig. 3). Diatoms and cyanobacteria account for 27% and 28% of GPP, respectively. Net primary productivity is balanced largely by the direct utilization of phytoplankton by zooplankton grazers. In the MN solution, only the "AUT" group produces excess ungrazed biomass that passes directly to a detrital pool, and this flux is only 9% of group NPP. While cyanobacteria net production is grazed completely by protozoans, mesozooplankton exert a significant proportion of the grazing pressure on eukaryotic phytoplankton (47% of total grazing on diatoms and 31% on other autotrophs). Protozoan losses to respiration are high, accounting for more than half (55%, 70%, and 52% for pico-, nano-, and microzooplankton, respectively) of total carbon ingested. Larger zooplankton rely proportionally more on carnivory. Mesozooplankton, for example, derive 31% of their carbon requirements from other heterotrophs and occupy a mean trophic level of 2.29. Bacteria constitute a relatively small portion of protozoan diets (25%, 9%, and 1% for pico-, nano-, and microzooplankton) yet play a significant role in carbon flux, respiring 10% of GPP.

Export out of the ecosystem is split between horizontal advection of DOC, vertical sinking of POC, and energy transport through mesozooplankton to higher trophic levels. The *e*-ratio (ratio of vertical carbon flux to net primary productivity) predicted by the model is a moderate 10%. Some detritus comes directly from phytoplankton (27%), but most is formed as fecal carbon after digestive processing by the various zooplankton size classes. System flows indicate that the carbon export derives primarily from nondiatom eukaryotic phytoplankton (65%), with diatoms and cyanobacteria contributing 16% and 19%, respectively.

Our results depict an ecosystem that is strikingly different from that of the similarly structured model of Richardson et al. (2004). While this previous model predicted a phytoplankton community with production dominated by picophytoplankton, the present analysis is constrained by field data that establish that most production comes from eukaryotes. Cyanobacteria were completely grazed by protozoan grazers in our experimental data (Landry et al. 2010), while the Richardson et al. (2004) model suggested that over a quarter of picoplankton productivity was ungrazed and passed directly into the detrital pool (Table 4). Nonetheless, the two models produce similar estimates of the utilization of heterotrophic protists in the diets of mesozooplankton, and both suggest that carbon is exported from the system by DOC advection and by higher trophic levels in relatively similar amounts. Both models also suggest that detritus must form a significant portion of mesozooplankton diets, although the contribution is significantly higher for the EqPac model. Unlike the present results, however, the EqPac model required significant remineralization of detritus to DOC both to support the bacterioplankton community and as a sink for the large amount of detritus produced by ungrazed picophytoplankton. The EqPac model also produced lower vertical flux rates, as a result of measurement constraints placed on the EqPac model that were absent in the present analysis.

Model sensitivity—We tested the sensitivity of our ECO model to measurement inaccuracies using the Monte Carlo approach of simultaneously varying all measured values based on normal distributions created from their known means and standard errors (Table 4). To test the role of each measured input (taxon-specific net primary productivity, taxon-specific protozoan grazing, mesozooplankton grazing, *f*-ratio, size-fractionated protozoan biomass, bacterial biomass, and ^{14}C-PP) on the model outputs, we regressed each pair of inputs and outputs (Table 5). Many of the resulting relationships were trivial dependencies, such as the relationship of diatom GPP to measured diatom NPP. The strongest correlations, relating pico- and microzooplankton respiration to their respective biomasses, follow from the tendency of the MN algorithm to maximize the respiration of these groups. Likewise, the strong correlations among ^{14}C-PP and GPP, respiration, and excretion of all phytoplankton groups came from the model's tendency to minimize GPP. The most significant negative relationship was a surprising correlation between net primary productivity and respiration of the "other autotrophs." This pattern did not occur for other phytoplankton taxa and probably resulted from minimization of the largest model flow (gross production of other autotrophs; gAUtoAUT) when NPP of this group was significantly larger than NPP of diatoms and cyanobacteria. Dividing phytoplankton gross primary production as equitably as possible among groups led to an inequitable distribution of respiration, particularly when NPP of the dominant taxa was high. Many of these correlations thus tell us less about the actual behavior of the ecosystem than they do about the behavior of the MN model solution. Several of these relationships, for example, highlight the tendency of the MN solution to set biological constraints (e.g., GGE) to either the maximum or the minimum values

Table 4.   Solutions to the base ECO model. Flows are, by convention, from the first carbon pool to the second. Carbon pools are GPP of diatoms (gDI), GPP of other eukaryotic phytoplankton (gAU), GPP of cyanobacteria (gCY), diatoms (DIA), other eukaryotic autotrophs (AUT), cyanobacteria (CYA), heterotrophic picoflagellates (HPF), heterotrophic nanoflagellates (HNF), microzooplankton (MIC), mesozooplankton (MES), bacteria (BAC), detritus (DET), dissolved organic carbon (DOC), respiration (RES), and export from the ecosystem (EXT). EqPac is the equivalent solutions of the Richardson et al. (2004) model. ECO MN is the solution that minimizes the L_2 norm of our base ECO model. Monte Carlo mean and 95% confidence intervals (CIs) are derived from randomly drawing possible combinations of the measured inputs to the model. RW means and 95% CIs are drawn from an RW exploration of the possible solution space.

	Variable	EqPac*	ECO MN	ECO Monte Carlo, mean (CI)	ECO RW, mean (CI)
1	gDItoDIA	7.2–192	338	318(228–381)	255(188–325)
2	DIAtoRES	0.4–9.6	102	95.3(67–114)	50.5(13–92)
3	DIAtoHNF	na†	59.1	56.5(41–72)	46.9(4–81)
4	DIAtoMIC	2.4–61.2	23.9	21.0(4–36)	36.1(2–79)
5	DIAtoMES	0–42	73.0	70.2(24–115)	50.3(29–72)
6	DIAtoDET	4.0–75.6	0.0	20.6(0–95)	22.7(1–44)
7	DIAtoDOC	0.1–3.6	81.0	61.1(4–88)	48.4(6–84)
8	gAUtoAUT	155–431‡	579	596(521–681)	816(655–1023)
9	AUTtoRES	7.8–21.6‡	63.8	74.3(28–168)	164(46–286)
10	AUTtoHNF	23.2–140‡	176	173(139–207)	228(64–313)
11	AUTtoMIC	0–77.3‡	140	137(103–170)	87.6(3–252)
12	AUTtoMES	45.6–82.4‡	144	141(93–198)	167(145–188)
13	AUTtoDET	64.2–219.8‡	45.0	65.3(0–176)	22.3(1–44)
14	AUTtoDOC	2.9–5.0‡	10.1	10.3(8–12)	147(23–269)
15	gCYtoCYA	997–1181§	359	363(291–441)	333(245–424)
16	CYAtoRES	49.9–59.0§	108	108(85–132)	66.8(17–121)
17	CYAtoHPF	na‖	65.3	62.0(50–74)	59.5(3–143)
18	CYAtoHNF	445–1034§#	86.5	86.4(73–101)	83.7(5–176)
19	CYAtoMIC	2.0–106§	51.2	50.8(39–62)	59.8(3–157)
20	CYAtoDET	51.7–463§	0.0	13.0(0–60)	0.0(0–0)
21	CYAtoDOC	18.6–22.0§	48.6	47.0(4–101)	63.2(8–109)
22	HPFtoHNF	na‖	20.0	21.7(10–36)	22.4(1–58)
23	HPFtoMIC	na‖	0.0	0.0(0–0)	19.7(1–54)
24	HPFtoRES	na‖	45.0	45.0(30–60)	37.8(24–44)
25	HPFtoDET	na‖	8.2	8.9(7–11)	47.1(14–88)
26	HPFtoDOC	na‖	9.0	14.0(7–31)	25.6(12–40)
27	HNFtoMIC	0.0	0.0	0.0(0–0)	68.9(3–196)
28	HNFtoMES	106–235	40.0	42.3(36–52)	93.6(6–238)
29	HNFtoRES	369–543	280	289(250–335)	198(107–310)
30	HNFtoDET	68.3–112	40.0	41.2(36–48)	220(61–476)
31	HNFtoDOC	159–272	40.0	41.2(36–48)	107(53–186)
32	MICtoRES	4.3–30.6	114	114(104–123)	95.8(63–113)
33	MICtoMES	8.6–61.2	58.1	58.0(41–78)	95.7(35–177)
34	MICtoDET	4.3–30.6	21.7	22.0(20–25)	134(40–234)
35	MICtoDOC	4.3–30.6	23.2	26.7(20–46)	63.9(32–101)
36	MEStoRES	124–266	253	259(226–299)	179(97–294)
37	MEStoDET	41.0–66.6	36.2	37.2(33–43)	189(54–381)
38	MEStoDOC	57.1–94.7	36.2	37.2(33–43)	93.8(47–166)
39	BACtoRES	180–265	121	129(97–172)	423(256–596)
40	BACtoHPF	na‖	15.4	15.6(10–20)	33.1(2–90)
41	BACtoHNF	88.6–127#	36.6	40.0(28–53)	42.7(2–104)
42	BACtoMIC	0.0	1.3	4.9(0–11)	33.7(2–93)
43	BACtoDET	3.8–91.6	13.9	7.8(0–21)	20.8(1–61)
44	BACtoDOC	0–5.3	0.0	0.0(0–0)	276(11–709)
45	DETtoHPF	na‖	1.5	10.7(0–34)	60.0(3–150)
46	DETtoHNF	0–112#	22.6	34.7(9–73)	263(16–650)
47	DETtoMIC	0.0	0.0	5.3(0–32)	83.7(3–248)
48	DETtoMES	236–288	46.5	60.3(32–108)	148(6–446)
49	DETtoDOC	293–318	11.6	22.0(0–59)	62.2(2–199)
50	DOCtoBAC	300–450	189	196(158–243)	829(492–1251)
51	DOCtoEXT	206–304	71.2	64.0(35–89)	58.2(4–123)
52	DETtoEXT	22.8–42.0	82.8	85.0(50–120)	38.4(2–109)
53	MEStoEXT	164–266	36.2	39.4(34–50)	93.5(47–161)

* Solutions are the minimum and maximum of the four time series assessed by Richardson and Jackson (2004).
† The EqPac model did not allow (na) flow from diatoms to nano-sized protists.
‡ Combined values for the two nondiatom eukaryotic phytoplankton in the EqPac model.
§ The EqPac model's group of picophytoplankton includes picoeukaryotes but is functionally similar to our cyanobacteria compartment.
‖ The EqPac model had no heterotrophic picoflagellate (HPF) group.
Since the EqPac model had no HPF group, their protozoan group was equivalent to the sum of our HPF and HNF compartments.
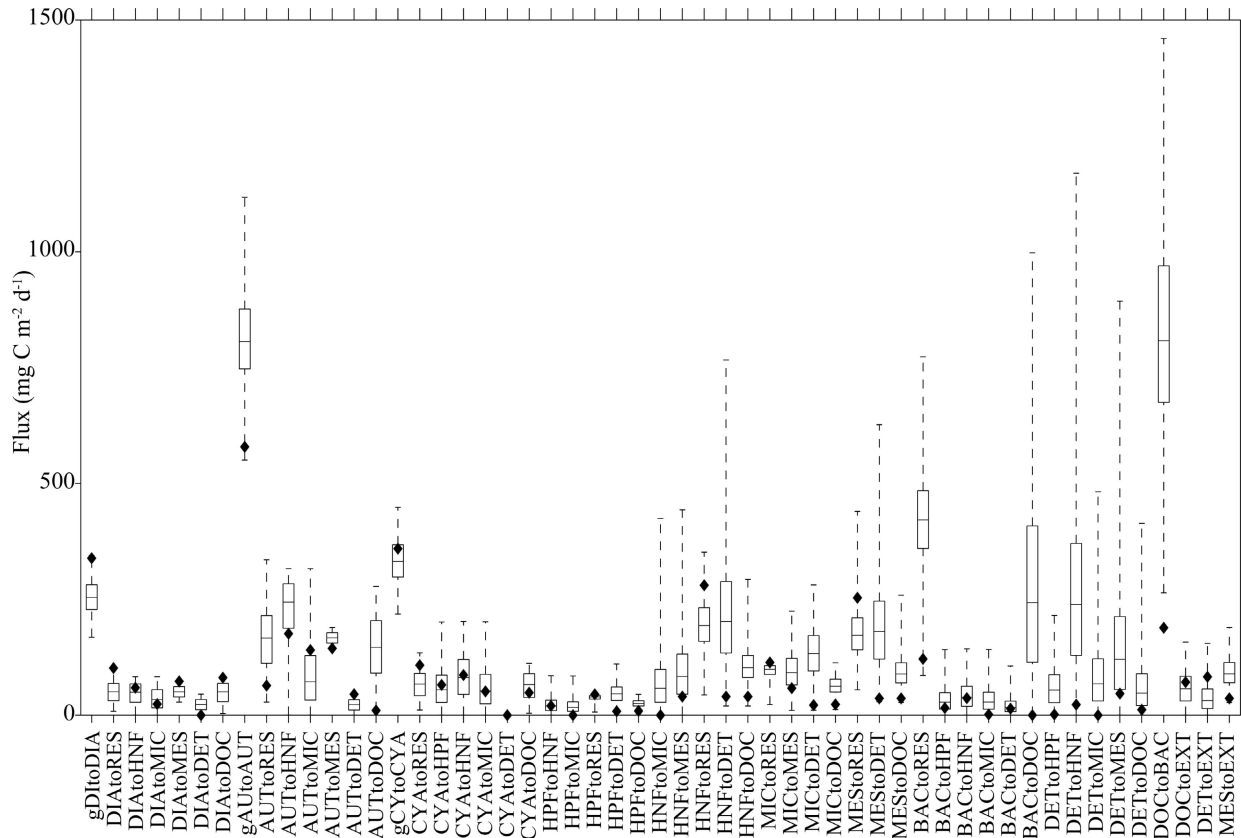
Fig. 3. RW exploration of the solution space. Boxes depict the middle two quartiles of an RW exploration of all the possible solutions that are consistent with the measured ecological rates and biological constraints imposed on the model. Dashed lines show the extreme values possible for each variable. Filled diamonds are the solutions obtained by using the common minimum norm technique. Note that for most variables, the MN solution is an extreme value that is poorly representative of the entire solution space.

allowed by the model (Table 3). Rather than settling on representative values that we might expect in the middle of any biologically possible range, the L_2 norm was minimized at the less likely extreme values; thus, the choice of constraint ranges had a large (and undesirable) effect on the solution (e.g., 5–50% GGE would produce significantly different results than 10–40%). In particular, the MN solution appeared to maximize respiration from the zooplankton groups in order to shunt energy out of the system as rapidly as possible (Fig. 3; Table 3).

RW exploration of the solution space—To explore the ensemble of solution vectors (the solution space) of our ECO model beyond the single MN result, we used an RW approach to sample the solutions that satisfied the biological constraints. We applied the RW algorithm until the average of the RW solutions converged on a value. The entire solution space was then used to calculate means and 95% confidence intervals for all flows (Table 4; Fig. 3), allowing us to compare with the MN solution, which was shown to be a biased representative of the greater solution space. Several of the most unconstrained flows in the model were pairs of flows allowing bidirectional fluxes of carbon between compartments (e.g., DOC to bacteria and bacteria to DOC). These paired flows were strongly related, with statistical correlations of 0.90, 0.78, and 0.67 for bidirec-

tional flows of bacteria to DOC, heterotrophic nanoflagellates to detritus, and mesozooplankton to detritus (flows between detritus and pico- or microzooplankton were better constrained because of the lower biomass of these grazers). The high correlations imply that the net uptakes or losses of carbon for each compartment were relatively well constrained and hence only weakly affected the other modeled flows, with the exception of increased ingestion leading to a concomitant increase in respiration.

As noted previously with regard to the biological constraints, the MN solution consistently used extreme values of the parameters (Fig. 3). To minimize the sum of squares, for example, the MN solution minimized the largest flow in the model (gAUtoAUT). Since NPP of the AUT group (nondiatom eukaryotic autotrophs) was a measured input to the model, this model behavior also minimized DOC excretion, which limited, in turn, the DOC uptake and the respiration of bacteria, leading to a relatively high bacterial GGE (36%).

The RW solution (Table 4) gave significantly higher GPP for the AUT group and lower for the DIA and CYA groups in comparison to the MN solution (Fig. 3). It allowed greater DOC exudation by the phytoplankton community, which was consumed by a less efficient assemblage of heterotrophic bacteria, which in turn contributed more to total community respiration. Grazing

Table 5. Correlations between model inputs (measured rates and standing stocks) and outputs (flows) that explain at least 30% of the variance in the modeled flow, as derived from the Monte Carlo error analysis. Signs show whether the relationship was positive or negative. Model inputs are biomass of heterotrophic picoflagellates (BioHPF), biomass of heterotrophic nanoflagellates (BioHNF), biomass of microzooplankton (BioMIC), biomass of mesozooplankton (BioMES), biomass of bacteria (BioBAC), ^{14}C primary productivity (^{14}C-PP), f-ratio (F-rat), NPP of diatoms (DiaNPP), NPP of other eukaryotic autotrophs (AutNPP), NPP of cyanobacteria (CyaNPP), protozoan grazing on diatoms, other eukaryotic autotrophs, and cyanobacteria (Diamzoogr, Autmzoogr, and Cyamzoogr, respectively) and mesozooplankton grazing (Mesgr).

Input	Output	R^2	Sign
BioHPF	HPFtoRES	1.00	+
BioMIC	MICtoRES	1.00	+
Autmzoogr	AUTtoHNF	0.97	+
Autmzoogr	AUTtoMIC	0.92	+
Diamzoogr	DIAtoHNF	0.84	+
Cyamzoogr	CYAtoMIC	0.83	+
Cyamzoogr	CYAtoHNF	0.82	+
Diamzoogr	DIAtoMIC	0.67	+
F-rat	DOCtoEXT	0.61	+
C-14PP	gCYtoCYA	0.55	+
C-14PP	CYAtoRES	0.52	+
C-14PP	CYAtoDOC	0.51	+
C-14PP	DOCtoBAC	0.50	+
DiaNPP	gDItoDIA	0.50	+
C-14PP	AUTtoRES	0.42	+
DiaNPP	DIAtoRES	0.41	+
F-rat	DETtoEXT	0.41	+
C-14PP	gAUtoAUT	0.40	+
Autmzoogr	MICtoDET	0.40	+
Cyamzoogr	CYAtoHPF	0.40	+
AutNPP	AUTtoDET	0.39	+
BioHPF	BACtoHPF	0.37	+
AutNPP	AUTtoRES	0.36	−
C-14PP	BACtoRES	0.36	+
CyaNPP	CYAtoDET	0.36	+
DiaNPP	DIAtoMES	0.33	+
AutNPP	gAUtoAUT	0.33	+
Cyamzoogr	CYAtoDET	0.32	−
C-14PP	DIAtoDOC	0.32	+
Autmzoogr	BACtoMIC	0.31	−
C-14PP	BACtoHNF	0.31	+
AutNPP	DETtoEXT	0.31	+

efficiently regulated the phytoplankton community with only 5% of NPP passing ungrazed into the detrital pool. Cyanobacteria were particularly well constrained in the experimental field data and were completely grazed by the protozoan community in the inverse analysis. Despite their lower NPP, diatoms contributed the largest ungrazed proportion of their production (15%) directly to detritus. Grazing on the total phytoplankton community was dominated by the heterotrophic protists (Fig. 4), although mesozooplankton contributed 38% and 35% of the total grazing pressure on diatoms and other eukaryotic phytoplankton, respectively. Omnivory or carnivory made up a significant fraction of the feeding of microzooplankton and especially mesozooplankton, while bacteria were a minor prey source for the zooplankton community. Detritus,

however, was an important food source, especially for heterotrophic nanoflagellates. Vertical export of detritus out of the ecosystem came primarily from grazer-derived detritus and was indirectly derived from the phytoplankton groups in rough proportion to their NPP, with eukaryotic phytoplankton dominating the signal (Fig. 5a). Less carbon was exported than in the MN solution, while more was transferred to higher trophic levels than allowed by the high respiratory losses imposed by the MN solution.

SF-Det model—Our alternative SF-Det inverse model differs mainly from the base ECO model in defining size-based trophic interaction for three size classes of detritus and by not allowing the smallest size class, the picodetritus pool of colloidal-sized (0.2–2-μm) particles, to sink. Overall, most results of the SF-Det model were very similar to those of the original ECO model (Table 6). However, the SF-Det modifications significantly affected utilization of detritus and its export from the system. SF-Det gave higher export than the base ECO model (Fig. 5b) because the abundant nanoflagellates were no longer allowed to graze large (>20-μm) detrital particles. The proportion of export derived indirectly from diatoms also increased at the expense of that derived from cyanobacteria. The direct contribution to sinking detritus was also significantly altered by the SF-Det model structure with the flux coming primarily from fecal pellets of micro- and mesozooplankton at the expense of the fecal debris (egested vacuole contents) produced by smaller protozoans (Fig. 5c,d).

Discussion

As applied to the analysis of ocean food webs, the great strength of inverse models is their use of objective techniques to resolve the flows in complex networks where many of the rate terms are undetermined by data. This does not mean, however, that inverse analyses necessarily produce reliable or even realistic portrayals of system flows under all circumstances. Here we show that applying a new and more constrained data set to an inverse model that was structurally similar to Richardson et al. (2004) led to substantially different solutions with regard to the role of picophytoplankton in the equatorial Pacific food web, the balance of phytoplankton growth by grazing processes, the pathways and flows of production to DOC and detritus, and the efficiency of bacterial growth. In the following sections, we consider how the results of these models can be influenced by several factors, including different solution schemes, subjective assumptions about critical model input terms, and alternate structures for export-relevant processes.

Inverse model solutions and biases—Studies based on inverse ecosystem analyses often neglect errors associated with the minimization scheme (Fig. 3; Table 4). While a solution set that minimizes the L_2 norm may be parsimonious in a mathematical sense, from an ecological perspective it imposes an additional structure on the solution that is not explicit in the applied equality and inequality constraints. In particular, the MN solution is achieved by maximizing respiratory losses of lower-level

grazers (Table 3) and minimizing the number of trophic links. In the Richardson et al. (2004, 2006) models, for example, this behavior contributed to low rates of DOC production by phytoplankton and hence the unrealistically high bacterial gross growth efficiencies noted by Landry (2009). The mean solution set, by averaging each flow from a random compilation of all vectors that solve both the equality and the inequality constraints, may consequently provide a simpler and perhaps more ecologically relevant answer to the underconstrained ecosystem model.

Model structure also has a large and overlooked effect on inverse ecosystem analysis. However, it is often difficult to assess a priori the level of complexity that is necessary to accurately depict the ecology of the system, and, in fact, the necessary complexity depends on the questions addressed. In the present example, for instance, the added complexity of size-fractionated detritus did not seem to matter very much for assessing the major flows among most biological components of the equatorial Pacific ecosystem. However, it did significantly alter conclusions that can be made about the origins of carbon export from the euphotic zone (Fig. 5). Thus, when commonalities are found in the behaviors of disparate food webs and especially when those results differ greatly from conventional understanding, it is important to assess the role that the model structure and assumptions may have played in forcing the solutions.

Comparison to EqPac—Based on inverse analysis of data from the US JGOFS EqPac Program as well as similar findings for the Arabian Sea (Richardson et al. 2004, 2006), Richardson and Jackson (2007) reported that picophytoplankton production was directly and indirectly responsible for most (73%) of the carbon export in these two open-ocean ecosystems. In retrospect, this conclusion hangs critically on the assumption that production can be assigned to different size fractions based on their contributions to size-fractionated Chl *a*. For the EqPac program, which lacked a coherent database on plankton carbon biomass from microscopy, the assumed chlorophyll–production relationship led to picophytoplankton making up an average of 73% (SD = 9%) of the total community primary production (PP) in the four cruise scenarios that were modeled. In contrast, our new data for the equatorial Pacific, based on robust microscopical analyses and carbon-based estimates of growth rates, put total picophytoplankton production at 27% of PP, with 23% originating as the production of cyanobacteria (Table 1), *Prochlorococcus* and *Synechococcus*, the two components that we have explicitly considered here. Our new model based on this data consequently shows a large decline in the export flux that can be attributed to picophytoplankton populations, but the difference principally reflects the former assumption vs. the new field-estimated rates that determine the input terms for size-structured production. In other respects, data from the EqPac and EB cruises do not show substantial differences. For example, a large fraction, 75–80%, of Chl *a* passed through 3-μm filters on the EB cruises (Balch et al. 2010). The mean estimate of phytoplankton production consumed directly by protists on the EqPac
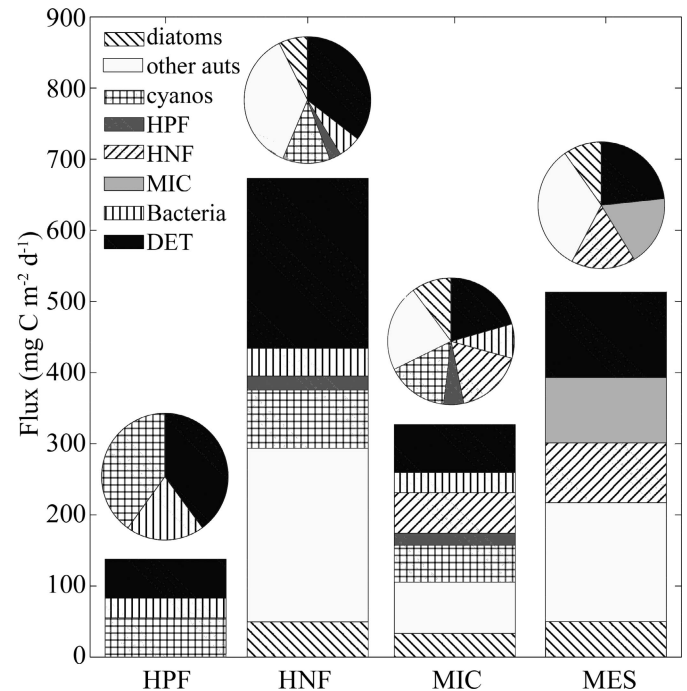

Fig. 4. Grazer diets. Bars show the RW solutions for the flux of carbon to each grazer from each of its prey groups. Pie charts show the composition of each grazer's diet for easier comparison.

cruises (88% of PP; Landry et al. 1997) was even higher than the 70% determined for EB cruises (Landry et al. 2010). As noted previously, the uncoupled growth and grazing in the Richardson et al. (2004) model was artificially imposed, in contradiction to direct field measurements from the EqPac study (Verity et al. 1996*b*). It appears, therefore, that the strongly different behaviors of the EqPac and our base ECO inverse models with regard to picophytoplankton flows to detritus and DOC arise not from major changes in the equatorial Pacific between EqPac and EB studies but from the carbon cycling challenges of the former model in meeting system steady-state model constraints when an unrealistic amount of production is assigned to the smallest size fraction.

Although the magnitude of the export flux contribution of picophytoplankton was exaggerated in the Richardson et al. (2004) model, according to new data on taxon-specific contributions to primary production in the equatorial Pacific, our revised model provides support for a central finding of the previous results. The RW solution of our base ECO model indicates, for example, that cyanobacteria production accounted for 23% of C export (Fig. 5a), the same as their percentage contribution to production, as predicted by the *proportionality* tenet of Richardson and Jackson (2007). Thus, an important part of their challenge to conventional expectations of phytoplankton size–export relationships is retained in the results of the new model with well-constrained biomass and rate data. Nonetheless, since picophytoplankton production in the Richardson et al. (2004, 2006) models was assigned according to a biomass proxy, size-fractionated chlorophyll, it needs to be noted that the 23% cyanobacteria contribution to export in the present

Table 6. SF-Det model solutions. Variables are the same as in Table 3 but calculated for the SF-Det model. PDT, NDT, and MDT are picodetritus, nanodetritus, and microdetritus, respectively. Equivalent solutions for the base ECO model are shown for comparison. Note that all flows not involving detritus were similar between the two models.

| | | Min norm solutions | | RW solutions | | |
| | | | | | 95% confidence | |
	Variable	SF-Det	Base ECO	SF-Det mean	interval	Base ECO
1	gDItoDIA	338	339	256	189–325	255
2	DIAtoRES	101	102	51.0	13–93	50
3	DIAtoHNF	55.8	59	47.0	4–81	47
4	DIAtoMIC	27.2	24	36.0	2–79	36
5	DIAtoMES	73.0	73	51.2	33–68	50
6	DIAtoNDT	0.0		11.2	1–31	
7	DIAtoMDT	0.0		10.6	1–30	
8	DIAtoDOC	80.5	81	48.9	6–84	48
9	gAUtoAUT	580	579	836	664–1045	816
10	AUTtoRES	65.2	64	178	50–297	164
11	AUTtoHNF	172	176	239	91–313	228
12	AUTtoMIC	144	140	76.8	3–225	88
13	AUTtoMES	144	144	166	149–184	167
14	AUTtoNDT	21.6		12.1	1–32	
15	AUTtoMDT	23.4		11.1	1–31	
16	AUTtoDOC	10.1	10	153	24–270	147
17	gCYtoCYA	359	359	331	245–422	333
18	CYAtoRES	108	108	65.8	17–120	67
19	CYAtoHPF	61.7	65	56.9	3–140	60
20	CYAtoHNF	85.0	86	90.6	7–180	84
21	CYAtoMIC	56.3	51	55.5	2–151	60
22	CYAtoPDT	0.0		0.0	0	
23	CYAtoDOC	48.0	49	62.5	8–109	63
24	HPFtoHNF	21.4	20	21.7	1–56	22
25	HPFtoMIC	0.0	0	19.1	1–53	20
26	HPFtoRES	45.0	45	37.4	23–44	38
27	HPFtoPDT	8.3		46.4	13–88	
28	HPFtoDOC	8.3	9	24.9	12–40	26
29	HNFtoMIC	0.0	0	65.2	3–180	69
30	HNFtoMES	40.3	40	77.5	5–185	94
31	HNFtoRES	282	280	172	103–266	197
32	HNFtoPDT	40.3		211	68–402	
33	HNFtoDOC	40.3	40	94.2	52–157	107
34	MICtoRES	114	114	99.9	73–113	96
35	MICtoMES	59.8	58	97.5	42–178	96
36	MICtoNDT	40.5		173	84–251	
37	MICtoDOC	23.8	23	67.1	38–102	64
38	MEStoRES	248	253	162	95–256	179
39	MEStoMDT	35.4		194	68–346	
40	MEStoDOC	35.4	36	85.9	46–146	94
41	BACtoRES	124	121	468	300–635	423
42	BACtoHPF	14.1	15	35.4	2–93	33
43	BACtoHNF	37.4	37	41.7	2–103	43
44	BACtoMIC	8.8	1	33.2	2–92	34
45	BACtoPDT	6.9		21.1	1–60	
46	BACtoDOC	0.0	0	253	10–661	276
47	PDTtoHPF	7.2		57.3	3–145	
48	PDTtoHNF	30.6		122	5–347	
49	NDTtoHNF	0.0		56.5	2–158	
50	PDTtoMIC	1.9		56.1	2–169	
51	NDTtoMIC	0.0		40.1	2–127	
52	MDTtoMIC	0.0		55.6	2–160	
53	NDTtoMES	19.3		44.0	2–134	
54	MDTtoMES	17.6		90.8	3–274	
55	PDTtoDOC	15.8		42.6	2–134	
56	NDTtoDOC	0.0		31.5	1–103	
57	MDTtoDOC	0.0		40.8	2–126	

Table 6. Continued.

| | | Min norm solutions | | RW solutions | | |
	Variable	SF-Det	Base ECO	SF-Det mean	95% confidence interval	Base ECO
58	DOCtoBAC	192	189	852	533–1260	829
59	DOCtoEXT	70.6	71	52.4	3–114	58
60	NDTtoEXT	42.9		24.2	1–77	
61	MDTtoEXT	41.2		28.9	1–87	
62	MEStoEXT	35.4	36	84.6	46–145	93

study falls far short of their contribution to phytoplankton biomass (36%). Thus, picophytoplankton contribution to biomass does not substitute for contribution to net production in the proportionality finding. The inclusion of size-structured detritus in our SF-Det model also led to a greater export role for larger cells like diatoms at the expense of picophytoplankton (Fig. 5b). Even under this model construction that did not allow direct sinking of picodetritus, however, picophytoplankton were responsible for producing 18% of the exported carbon (three-fourths of the percentage predicted by the proportionality argument and half their contribution to carbon biomass).

A strong growth-grazing balance for picophytoplankton populations, with protists applying essentially all of the grazing pressure, follows directly from the experimental measurements (Landry et al. 2010; Selph et al. 2010) and is a consistent feature of both forms of our model and minimization schemes. Thus, unlike the Richardson et al. (2004, 2006) analyses, the export of picophytoplankton-based production cannot be said to be unrealistically enhanced by a large fraction escaping consumption in the microbial food web and passing directly to detritus. As an output, our estimates of the *e*-ratio (export of 5.7% of ^{14}C-PP with the base ECO model and 7.9% with the SF-Det model), which was left unconstrained by data in the present analyses, agree well with the regionwide EqPac estimates of < 5–10% from Buesseler et al. (1995).

Complete grazing of cyanobacteria by protists may seem at odds with model results that show picophytoplankton

contributing to export in proportion to their production. In both the EqPac and our base ECO models, however, this proportionality derives from the implicit assumption that there is complete and immediate homogenization of everything that enters the detrital pool, essentially allowing protozoan egesta to sink as rapidly as mesozooplankton fecal pellets. The maintenance of semiproportionality after inclusion of detrital size classes (picophytoplankton contribute 18% of export compared to 23% of NPP) in our SF-Det model is a more intriguing result, especially since mesozooplankton, which provide the dominant mechanism for producing sinking particles, are not allowed to graze on picoplankton. The relevant insight from field-measured rates is that protists also consume most (60%) eukaryotic phytoplankton production (Fig. 6). Thus, the primary fates of pico- and larger phototrophs are not nearly as distinct as the traditional dichotomy between the ''classical food chain'' and the ''microbial loop.'' In fact, mesozooplankton derive only 44% of their ingestion from phytoplankton in the RW solution of our SF-Det model, with an additional 34% derived from grazing on protozoans and the remainder comprised of detrital material (Fig. 4). Thus, the contribution of cyanobacteria to export is derived from ecosystem linkages not readily assessed by traditional techniques (Fig. 7). It is also important to note that proportionality is found only for the RW solution to the SF-Det model. The unrealistically high respiratory demands of the MN solution do not allow efficient energy transfer up the food chain.
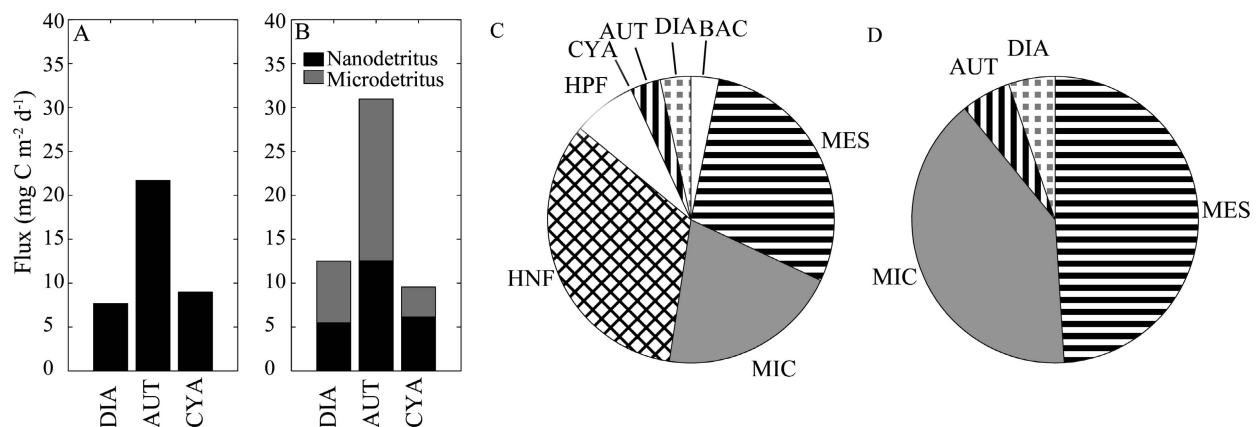

Fig. 5. Sources of particulate flux out of the euphotic zone. (A, B) The amount of sinking carbon export supported indirectly by each of the three primary producers based on (A) the base ECO model and (B) the SF-Det model. (B) The carbon flux is broken into flux through nano- and microdetritus. (C, D) Direct contributions to sinking carbon export according to the (C) ECO and (D) SF-Det models.
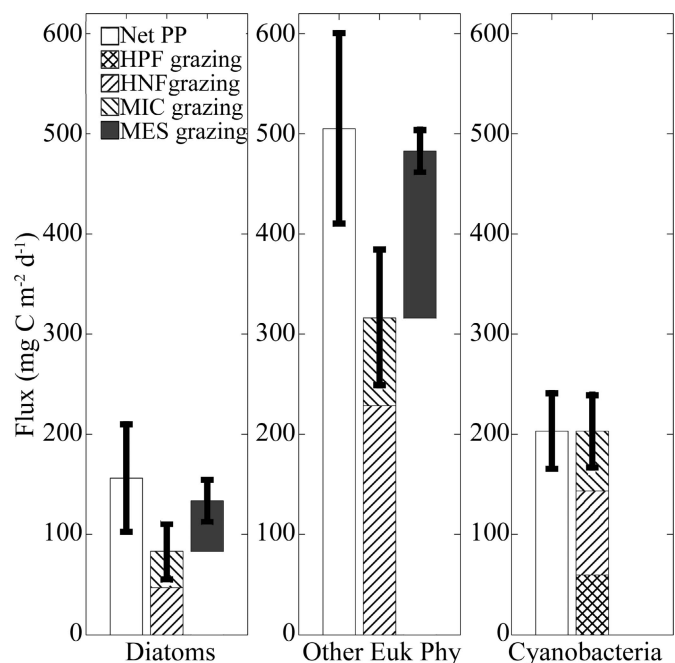
Fig. 6. Grazing balance. The figure shows the balance between growth and grazing for diatoms, other eukaryotic phytoplankton, and cyanobacteria. Error bars for net primary productivity and protozoan grazing are the 95% confidence limits for the measured rates, while error bars for the mesozooplankton grazing were derived from the 95% confidence limits of the RW exploration of the solution space. Note the strong correlation between growth and community grazing for each phytoplankton group. Results are all from the base ECO model and were very similar to the equivalent results from the SF-Det model.

While sediment traps cannot trace the primary source of exported carbon, their contents provide a glimpse of the nature of sinking particles. Rodier and Le Borgne (1997) utilized flow cytometry, microscopy, and pigment analyses to assess the contents of drifting sediment traps deployed for a week on the equator at 150°W, finding that intact picophytoplankton made up only a tiny fraction of the carbon flux. The dominant signal was from marine snow and fecal pellets, which were numerically dominated by particles in the 20–100-μm size class. Pigment analyses suggested that only 4% of POC flux came from intact phytoplankton, while 12% came from recent herbivory. Similarly, sediment traps deployed at 140°W during EqPac had very low ratios of chlorophyll to phaeopigment (Newton and Murray 1994), indicative of a low export percentage of intact cells. These values compare favorably with our model predictions of direct flux from phytoplankton (7% for the RW solution of the base ECO model and 11% for the SF-Det model) and from the fecal pellets of herbivorous zooplankters (41% for ECO and 36% for SF-Det), with the caveat that the percent pigmented ratio of detritus should decrease through microbial activity and coprophagy as particles sink to the depths of the traps.

Dam et al. (1995) determined that mesozooplankton fecal carbon production alone could have supported all the vertical flux measured during JGOFS EqPac cruises. Consistent with this, our model suggests that fecal matter makes up the dominant pathway by which carbon leaves the system (Fig. 5c,d), as a by-product of the growth-grazing balance of the euphotic zone (Fig. 6), but that most is reworked or degraded through coprophagy or dissolution to DOC. The SF-Det model indicated that food chain length to larger zooplankton was a major determinant of the efficiency of carbon export from the system, unlike the base ECO model, which, by treating all detrital particles equally, unrealistically allowed protozoan egesta to sink as rapidly as mesozooplankton pellets.

Processes altering export rates—Like all models, ours oversimplifies complex ecology and excludes processes deemed to be of lesser importance or poorly assessed by field measurements. The absence of phytoplankton density measurements means, for example, that we could not consider the inorganic ballasting effect of siliceous and calcareous planktonic taxa (Armstrong et al. 2002), which can significantly increase flux rates, thereby enhancing the export roles of diatoms and coccolithophores (both directly and by adding density to zooplankton egesta). We have likewise not explicitly accounted for particle aggregation (Alldredge and Gotschalk 1989; Walsh and Gardner 1992; Jackson 2001), which involves both phytoplankton and bacterial interactions (Passow et al. 1994, 2001) and provides an alternate pathway for flux of smaller particles to depth. In addition, the model does not expressly consider pelagic tunicates, like salps, which can efficiently pack cyanobacteria into rapidly sinking fecal pellets (Pfann-kuche and Lochte 1993), or appendicularians, which concentrate picophytoplankton in the mucus web feeding nets of their discarded houses (Robison et al. 2005). By the same token, however, the model does not consider active diel vertical migrations of mesozooplankton, which trans-port to depth substantial amounts of carbon derived primarily from large prey (Dam et al. 1995; Zhang and Dam 1997). All these represent poorly constrained mech-anisms that can alter the relative contributions of small and large phytoplankton to total system organic carbon export.

The SF-Det model illustrates, however, the importance of including size-fractionated detritus when assessing the origin of sinking detritus, although its equivalent treatment of nano- and microdetritus with respect to sinking is still simplistic. Microsized fecal pellets produced by mesozoo-plankton are likely to sink much faster than smaller detrital particles, suggesting that these large fecal pellets may make up an even greater proportion of exported material than the 49% suggested by the SF-Det model. In fact, 20–100-μm particles (equivalent to a portion of our microdetrital group) were the primary fecal material in the equatorial sediment traps examined by Rodier and Le Borgne (1997). Our model's microdetritus was composed primarily of mesozooplankton fecal pellets and supported by the production of eukaryotic phytoplankton with only minor contribution from cyanobacteria (Fig. 5). While this highlights the importance of an accurate treatment of detritus, better constraints on this nonliving fraction will depend on experimental measurement by techniques such as detrital stains (Verity et al. 1996a) and sediment traps paired with polyacrylamide gels (Lundsgaard 1995).
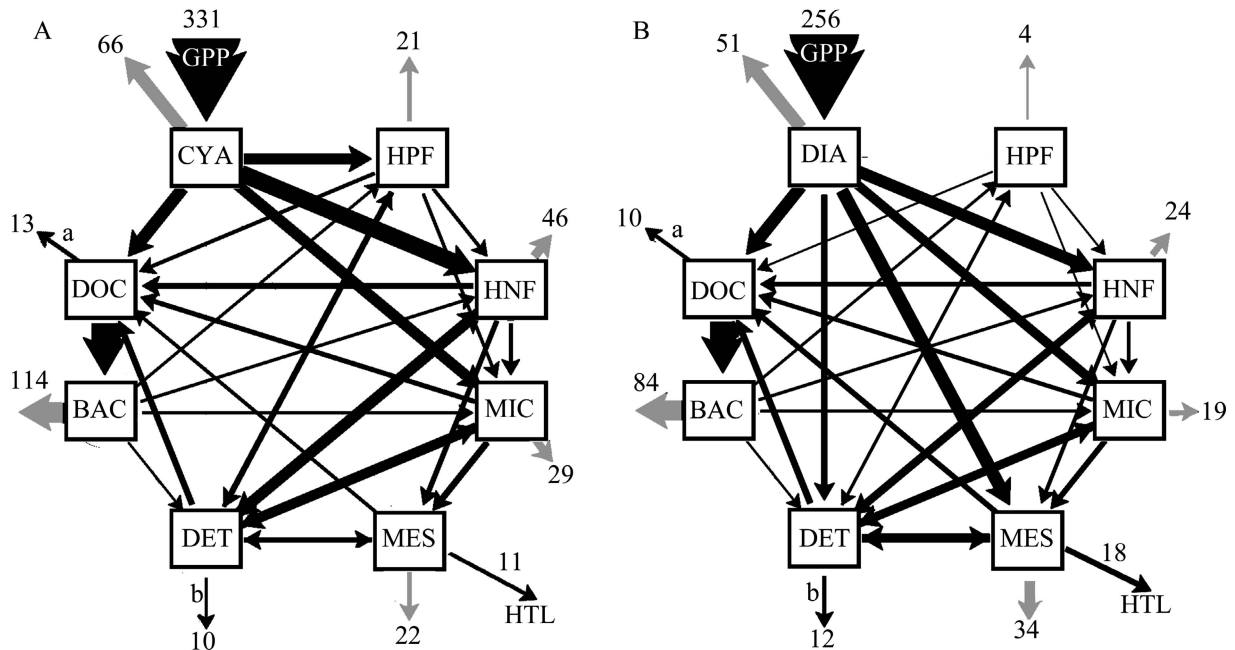
Fig. 7. Carbon fluxes supported by (A) cyanobacterial and (B) diatom production in the RW solution to the SF-Det model. Widths are proportional to magnitude. Flows into (GPP) and out of (respiration [gray], flux to higher trophic levels [HTL], lateral advection of DOC [a], and vertical flux [b]) the model are given in units of mg C m^{-2} d^{-1}. For ease of visualization, all detrital size classes are combined in the figure, and only the net flow of DOC to bacteria is depicted. Note the similarity in the ecosystem structure supported by cyanobacteria and diatoms with most energy dissipated by respiration of the "microbial loop" regardless of the primary carbon source. Fluxes were calculated using the indirect flow methods of Hannon (1973).

In summary, we found that many of the unexpected results of the Richardson et al. (2004) inverse model of the equatorial Pacific—namely, the picophytoplankton dominance of export, the imbalance of phytoplankton growth and grazing processes, the unusual pathways and flows of production to DOC and detritus, and the high efficiency of bacterial growth—were largely resolved by better data constraints on biomass and rates for the full euphotic zone and the taxonomic and size-class origins of primary production and by solution schemes that avoided the extremes of the minimal L_2 norm. Proportionality of net production and export contributions among phytoplankton size classes, a central conclusion of Richardson and Jackson (2007), remained a robust feature of the base model despite the previously mentioned refinements. We have shown, however, that this conclusion is sensitive to the treatment of detrital size classes; thus, this is an area where insights from direct field measurements and model development would be useful. Future progress in understanding the roles of different taxa in export processes also clearly requires data sets that more directly and quantitatively link the growth and trophic dynamics of different functional groups in the euphotic zone to their incorporation into exported material so that we might usefully compare model predictions to measurements and highlight potentially important missing processes.

References

ALLDREDGE, A. L., AND C. C. GOTSCHALK. 1989. Direct observations of the mass flocculation of diatom blooms: Characteristics, settling velocities and formation of diatom aggregates. Deep-Sea Res. **36:** 159–171.

ARMSTRONG, R. A., C. LEE, J. I. HEDGES, S. HONJO, AND S. G. WAKEHAM. 2002. A new, mechanistic model for organic carbon fluxes in the ocean based on the quantitative association of POC with ballast minerals. Deep-Sea Res. II **49:** 219–236, doi:10.1016/S0967-0645(01)00101-1

AZAM, F., T. FENCHEL, J. G. FIELD, J. S. GRAY, L. A. MEYER-REIL, AND F. THINGSTAD. 1983. The ecological role of water-column microbes in the sea. Mar. Ecol. Prog. Ser. **10:** 257–263, doi:10.3354/meps010257

BALCH, W. M., A. J. POULTON, D. T. DRAPEAU, B. C. BOWLER, L. A. WINDECKER, AND E. S. BOOTH. 2010. Zonal and meridional patterns of phytoplankton biomass and carbon fixation in the equatorial Pacific Ocean, between 110°W and 140°W. Deep-Sea Res. II **57,** doi:10.1016/j.dsr2.2010.08.004

BENDER, M., J. ORCHARDO, M. L. DICKSON, R. BARBER, AND S. LINDLEY. 1999. In vitro O_2 fluxes compared with ^{14}C production and other rate terms during the JGOFS Equatorial Pacific experiment. Deep-Sea Res. I **46:** 637–654, doi:10.1016/S0967-0637(98)00080-6

BROWN, S. L., M. R. LANDRY, R. T. BARBER, L. CAMPBELL, D. L. GARRISON, AND M. M. GOWING. 1999. Picophytoplankton dynamics and production in the Arabian Sea during the 1995 Southwest Monsoon. Deep-Sea Res. II **46:** 1745–1768, doi:10.1016/S0967-0645(99)00042-9

———, ———, K. E. SELPH, E. J. YANG, Y. M. RII, AND R. R. BIDIGARE. 2008. Diatoms in the desert: Plankton community response to a mesoscale eddy in the subtropical North Pacific. Deep-Sea Res. II **55:** 1321–1333, doi:10.1016/j.dsr2.2008.02.012

BUESSELER, K. O., J. A. ANDREWS, M. C. HARTMAN, R. BELASTOCK, AND F. CHAI. 1995. Regional estimates of the export flux of particulate organic carbon derived from thorium-234 during the JGOFS EqPac Program. Deep-Sea Res. II **42:** 777–804, doi:10.1016/0967-0645(95)00043-P

CHRISTENSEN, V., AND D. PAULY. 1992. ECOPATH II: A software for balancing steady-state ecosystem models and calculating network characteristics. Ecol. Model. **61:** 169–185, doi:10.1016/0304-3800(92)90016-8

DAM, H. G., X. S. ZHANG, M. BUTLER, AND M. R. ROMAN. 1995. Mesozooplankton grazing and metabolism at the equator in the central Pacific: Implications for carbon and nitrogen fluxes. Deep-Sea Res. II **42:** 735–756, doi:10.1016/0967-0645(95)00036-P

DÉCIMA, M., M. R. LANDRY, AND R. R. RYKACZEWSKI. 2010. Broad-scale patterns in mesozooplankton biomass and grazing in the eastern equatorial Pacific. Deep-Sea Res. II **57,** doi:10.1016/j.dsr2.2010.08.006

DICKSON, M. L., J. ORCHARDO, R. T. BARBER, J. MARRA, J. J. MCCARTHY, AND R. N. SAMBROTTO. 2001. Production and respiration rates in the Arabian Sea during the 1995 Northeast and Southwest Monsoons. Deep-Sea Res. II **48:** 1199–1230, doi:10.1016/S0967-0645(00)00136-3

DUCKLOW, H. W., H. L. QUINBY, AND C. A. CARLSON. 1995. Bacterioplankton dynamics in the equatorial Pacific during the 1992 El-Niño. Deep-Sea Res. II **42:** 621–638, doi:10.1016/0967-0645(95)00022-I

DUGDALE, R. C., AND F. P. WILKERSON. 1998. Silicate regulation of new production in the equatorial Pacific upwelling. Nature **391:** 270–273, doi:10.1038/34630

FROST, B. W., AND N. C. FRANZEN. 1992. Grazing and iron limitation in the control of phytoplankton stock and nutrient concentration: A chemostat analog of the Pacific equatorial upwelling zone. Mar. Ecol. Prog. Ser. **83:** 291–303, doi:10.3354/meps083291

GARRISON, D. L., AND OTHERS. 2000. Microbial food web structure in the Arabian Sea: A US JGOFS study. Deep-Sea Res. II **47:** 1387–1422, doi:10.1016/S0967-0645(99)00148-4

GORSKY, G., M. J. CHRETIENNOT-DINET, J. BLANCHOT, AND I. PALAZZOLI. 1999. Picoplankton and nanoplankton aggregation by appendicularians: Fecal pellet contents of *Megalocercus huxleyi* in the equatorial Pacific. J. Geophys. Res. Oceans **104:** 3381–3390, doi:10.1029/98JC01850

HANNON, B. 1973. Structure of ecosystems. J. Theor. Biol. **41:** 535–546, doi:10.1016/0022-5193(73)90060-X

HIROSE, M., T. KATANO, AND S. I. NAKANO. 2008. Growth and grazing mortality rates of Prochlorococcus, Synechococcus and eukaryotic picophytoplankton in a bay of the Uwa Sea, Japan. J. Plankton Res. **30:** 241–250, doi:10.1093/plankt/fbm101

JACKSON, G. A. 2001. Effect of coagulation on a model planktonic food web. Deep-Sea Res. I **48:** 95–123, doi:10.1016/S0967-0637(00)00040-6

———, N. NIQUIL, A. BURD, AND T. L. RICHARDSON. 2001. Ecosystem Modeling Group Software. Inverse model code. College Station (TX): Texas A&M Univ, Available from http://oceanz.tamu.edu/~ecomodel/Software/invmodel/invmodel.html

KIRCHMAN, D. L., J. H. RICH, AND R. T. BARBER. 1995. Biomass and biomass production of heterotrophic bacteria along 140°W in the equatorial Pacific—effect of temperature on the microbial loop. Deep-Sea Res. II **42:** 603–619, doi:10.1016/0967-0645(95)00021-H

KONES, J. K., K. SOETAERT, D. VAN OEVELEN, AND J. O. OWINO. 2009. Are network indices robust indicators of food web functioning? A Monte Carlo approach. Ecol. Model. **220:** 370–382, doi:10.1016/j.ecolmodel.2008.10.012

LAMBORG, C. H., AND OTHERS. 2008. The flux of bio- and lithogenic material associated with sinking particles in the mesopelagic "twilight zone" of the northwest and north central Pacific Ocean. Deep-Sea Res. II **55:** 1540–1563, doi:10.1016/j.dsr2.2008.04.011

LANDRY, M. R. 2009. Grazing processes and secondary production in the Arabian Sea: A simple food web synthesis with measurement constraints, p. 133–146. *In* J. D. Wiggert, R. R. Hood, S. W. A. Naqvi, K. H. Brink, and S. L. Smith [eds.], Indian Ocean biogeochemical processes and ecological variability. AGU Monograph. American Geophysical Union.

———, H. AL-MUTAIRI, K. E. SELPH, S. CHRISTENSEN, AND S. NUNNERY. 2001. Seasonal patterns of mesozooplankton abundance and biomass at Station ALOHA. Deep-Sea Res. II **48:** 2037–2061, doi:10.1016/S0967-0645(00)00172-7

———, S. L. BROWN, J. NEVEUX, C. DUPOUY, J. BLANCHOT, S. CHRISTENSEN, AND R. R. BIDIGARE. 2003. Phytoplankton growth and microzooplankton grazing in high-nutrient, low-chlorophyll waters of the equatorial Pacific: Community and taxon-specific rate assessments from pigment and flow cytometric analyses. J. Geophys. Res. Oceans **108:** 8142, doi:10.1029/2000JC000744

———, J. CONSTANTINOU, M. LATASA, S. L. BROWN, R. R. BIDIGARE, AND M. E. ONDRUSEK. 2000. Biological response to iron fertilization in the eastern equatorial Pacific (IronEx II). III. Dynamics of phytoplankton growth and microzooplankton grazing. Mar. Ecol. Prog. Ser. **201:** 57–72, doi:10.3354/meps201057

———, K. E. SELPH, A. G. TAYLOR, M. DÉCIMA, W. M. BALCH, AND R. R. BIDIGARE. 2010. Phytoplankton growth, grazing and production balances in the HNLC equatorial Pacific. Deep-Sea Res. II **57,** doi:10.1016/j.dsr2.2010.08.011

———, AND OTHERS. 1997. Iron and grazing constraints on primary production in the central equatorial Pacific: An EqPac synthesis. Limnol. Oceanogr. **42:** 405–418, doi:10.4319/lo.1997.42.3.0405

LI, W. K. W., D. V. S. RAO, W. G. HARRISON, J. C. SMITH, J. J. CULLEN, B. IRWIN, AND T. PLATT. 1983. Autotrophic picoplankton in the tropical ocean. Science **219:** 292–295, doi:10.1126/science.219.4582.292

LOCHTE, K., AND C. M. TURLEY. 1988. Bacteria and cyanobacteria associated with phytodetritus in the deep sea. Nature **333:** 67–69, doi:10.1038/333067a0

LUNDSGAARD, C. 1995. Use of a high viscosity medium in studies of aggregates, p. 141–152. *In* S. Floderus, A.-S. Heisakanen, M. Oleson, and P. Wassmann [eds.], Sediment trap studies in the Nordic countries 3. Proceedings of the Symposium on Seasonal Dynamics of Planktonic Ecosystem and Sedimentation in Coastal Nordic Waters.

MENDEN-DEUER, S., AND E. J. LESSARD. 2000. Carbon to volume relationships for dinoflagellates, diatoms, and other protist plankton. Limnol. Oceanogr. **45:** 569–579, doi:10.4319/lo.2000.45.3.0569

NEWTON, J., AND J. MURRAY. 1994. Comparison of sinking particulate material in the central equatorial Pacific measured during the EqPac US-JGOFS field year. EOS, Transactions, American Geophysical Union **75:** 82, doi:10.1029/94EO00492

OLSEN, Y., AND OTHERS. 2006. A comparative study of responses in planktonic food web structure and function in contrasting European coastal waters exposed to experimental nutrient addition. Limnol. Oceanogr. **51:** 488–503, doi:10.4319/lo.2006.51.1_part_2.0488

PARKER, A. E., F. P. WILKERSON, R. C. DUGDALE, A. MARCHI, V. HOGUE, M. R. LANDRY, AND A. G. TAYLOR. 2010. Spatial patterns of nitrogen uptake and phytoplankton in the equatorial upwelling zone (110°W–140°W) during 2004 and 2005. Deep-Sea Res. II **57**, doi:10.1016/j.dsr2.2010.08.013

PASSOW, U., A. L. ALLDREDGE, AND B. E. LOGAN. 1994. The role of particulate carbohydrate exudates in the flocculation of diatom blooms. Deep-Sea Res. I **41:** 335–357, doi:10.1016/0967-0637(94)90007-8

———, R. F. SHIPE, A. MURRAY, D. K. PAK, M. A. BRZEZINSKI, AND A. L. ALLDREDGE. 2001. The origin of transparent exopolymer particles (TEP) and their role in the sedimentation of particulate matter. Cont. Shelf Res. **21:** 327–346, doi:10.1016/S0278-4343(00)00101-1

PFANNKUCHE, O., AND K. LOCHTE. 1993. Open ocean pelago-benthic coupling: Cyanobacteria as tracers of sedimenting salp feces. Deep-Sea Res. I **40:** 727–737, doi:10.1016/0967-0637(93)90068-E

RICHARDSON, T. L., AND G. A. JACKSON. 2007. Small phytoplankton and carbon export from the surface ocean. Science **315:** 838–840, doi:10.1126/science.1133471

———, ———, H. W. DUCKLOW, AND M. R. ROMAN. 2004. Carbon fluxes through food webs of the eastern equatorial Pacific: An inverse approach. Deep-Sea Res. I **51:** 1245–1274, doi:10.1016/j.dsr.2004.05.005

———, ———, ———, AND ———. 2006. Spatial and seasonal patterns of carbon cycling through planktonic food webs of the Arabian Sea determined by inverse analysis. Deep-Sea Res. II **53:** 555–575, doi:10.1016/j.dsr2.2006.01.015

ROBISON, B. H., K. R. REISENBICHLER, AND R. E. SHERLOCK. 2005. Giant larvacean houses: Rapid carbon transport to the deep sea floor. Science **308:** 1609–1611, doi:10.1126/science.1109104

RODIER, M., AND R. LE BORGNE. 1997. Export flux of particles at the equator in the western and central Pacific Ocean. Deep-Sea Res. II **44:** 2085–2113, doi:10.1016/S0967-0645(97)00092-1

SELPH, K. E., AND OTHERS. 2010. Spatially-resolved taxon-specific phytoplankton production and grazing dynamics in relation to iron distributions in the equatorial Pacific between 110 and 140°W. Deep-Sea Res. II **57**, doi:10.1016/j.dsr2.2010.08.014

SILVER, M. W., AND M. M. GOWING. 1991. The "particle" flux: Origins and biological components. Prog. Oceanogr. **26:** 75–113, doi:10.1016/0079-6611(91)90007-9

TAKAHASHI, M., AND P. K. BIENFANG. 1983. Size structure of phytoplankton biomass and photosynthesis in subtropical Hawaiian Waters. Mar. Biol. **76:** 203–211, doi:10.1007/BF00392736

TAYLOR, A. G., M. R. LANDRY, K. E. SELPH, AND E. J. YANG. 2010. Biomass, size structure and depth distributions of the microbial community in the eastern equatorial Pacific. Deep-Sea Res. II **57**, doi:10.1016/j.dsr2.2010.08.017

ULANOWICZ, R. E., AND J. J. KAY. 1991. A package for the analysis of ecosystem flow networks. Environmental Software **6:** 131–142, doi:10.1016/0266-9838(91)90024-K

VERITY, P. G., T. M. BEATTY, AND S. C. WILLIAMS. 1996a. Visualization and quantification of plankton and detritus using digital confocal microscopy. Aquat. Microb. Ecol. **10:** 55–67, doi:10.3354/ame010055

———, D. K. STOECKER, M. E. SIERACKI, AND J. R. NELSON. 1996b. Microzooplankton grazing of primary production at 140°W in the equatorial Pacific. Deep-Sea Res. II **43:** 1227–1255, doi:10.1016/0967-0645(96)00021-5

VÉZINA, A. F., AND T. PLATT. 1988. Food web dynamics in the ocean. 1. Best estimates of flow networks using inverse methods. Mar. Ecol. Prog. Ser. **42:** 269–287, doi:10.3354/meps042269

WAITE, A. M., K. A. SAFI, J. A. HALL, AND S. D. NODDER. 2000. Mass sedimentation of picoplankton embedded in organic aggregates. Limnol. Oceanogr. **45:** 87–97, doi:10.4319/lo.2000.45.1.0087

WALSH, I. D., AND W. D. GARDNER. 1992. A comparison of aggregate profiles with sediment trap fluxes. Deep-Sea Res. **39:** 1817–1834.

YOOL, A., A. P. MARTIN, C. FERNANDEZ, AND D. R. CLARK. 2007. The significance of nitrification for oceanic new production. Nature **447:** 999–1002, doi:10.1038/nature05885

ZHANG, X., H. G. DAM, J. R. WHITE, AND M. R. ROMAN. 1995. Latitudinal variations in mesozooplankton grazing and metabolism in the central tropical Pacific during the US JGOFS EqPac Study. Deep-Sea Res. II **42:** 695–714, doi:10.1016/0967-0645(95)00032-L

———, AND ———. 1997. Downward export of carbon by diel migrant mesozooplankton in the central equatorial Pacific. Deep-Sea Res. II **44:** 2191–2202, doi:10.1016/S0967-0645(97)00060-X